AIP | Applied Physics Letters

Microwave radiation power of relativistic electron beam with virtual cathode in the external magnetic field

S. A. Kurkin, A. E. Hramov, and A. A. Koronovskii

Citation: Appl. Phys. Lett. **103**, 043507 (2013); doi: 10.1063/1.4816471
View online: http://dx.doi.org/10.1063/1.4816471
View Table of Contents: http://apl.aip.org/resource/1/APPLAB/v103/i4
Published by the AIP Publishing LLC.

Microwave radiation power of relativistic electron beam with virtual cathode in the external magnetic field

S. A. Kurkin,[1,2,a)] A. E. Hramov,[1,2] and A. A. Koronovskii[1,2]
[1]*Saratov State University, Astrakhanskaja 83, Saratov 410012, Russia*
[2]*Saratov State Technical University, Politechnicheskaja 77, Saratov 410028, Russia*

(Received 8 May 2013; accepted 5 July 2013; published online 23 July 2013)

The study of the output power of the electromagnetic radiation of the relativistic electron beam (REB) with virtual cathode in the presence of external magnetic field has been found out. The typical dependencies of the output microwave power of the vircator versus external magnetic field have been analyzed by means of 3D electromagnetic simulation. It has been shown that the power of vircator demonstrates several maxima with external magnetic field growth. The characteristic features of the power behavior are determined by the conditions of the virtual cathode formation in the presence of the external transversal magnetic field and the REB self-magnetic fields. © *2013 AIP Publishing LLC*. [http://dx.doi.org/10.1063/1.4816471]

Beams of charged particles have great importance for understanding physical properties of plasmas, as well as for their technological applications. High power relativistic electron beams (REBs) are used in plasma heating, inertial fusion, high power microwave generation, and other. One of the most important directions of research in the high power vacuum and plasma electronics is the study of the virtual cathode (VC) oscillators (vircators) which attract great attention of scientific community.[1–8] The vircator is a microwave generator whose operation is based on the oscillations of the VC in the electron beam with the overcritical current.[1,4,9] Microwave oscillators with VC are perspective devices of high-power microwave electronics for the generation of the impulses of the wide-band microwave radiation due to their high output microwave radiation power, a simple construction (particularly, vircators can operate without the external focusing magnetic field), a possibility of a simple frequency tuning and regime switching.[2,4,10,11] All these circumstances increase the fundamental and applied importance of studies of the nonlinear dynamics of the electron beams with VC.

The oscillating VC is known to appear in the electron beam when the beam current exceeds a certain critical value, I_{cr} (so-called space charge limiting (SCL) current),[1,12] and the beam space charge is strong enough in order to form a potential barrier (VC) which reflects the electrons back to the injection plane. The mechanisms of the VC formation have been investigated in details in case of the one-dimensional (1D) electron beam motion (fully magnetized beam),[6,13,14] with the critical beam current value being analytically defined for this case in Ref. 12.

At the same time, a number of papers[15–21] have shown that the vircator output microwave power value demonstrates the complex behavior with the change of the system parameters, particularly with the growth of the external magnetic field. So, in Ref. 17 the experimental study of the dependencies of the output power of the microwave radiation of REB with VC in vircator on the external magnetic field has been provided. It has been shown that the typical dependence of the vircator microwave output power on the magnetic field demonstrates oscillating character with 2–3 peaks whose amplitude decreases with the magnetic field induction growth (see, for example, the typical output microwave power dependencies on the external magnetic field in Table in Ref. 17. It has been also demonstrated that for the strong magnetic fields the output power is saturated on the low power level. The same results have been also obtained in theoretical and experimental works[22–24]). However, the physical mechanisms of such power behavior are still uninvestigated in the most cases. So, the important problem in this field is the theoretical analysis of the behavior of microwave radiation output power of vircator under the external magnetic field variations and the study of the physical processes leading to its change. In particular, these studies are necessary for the analysis of contemporary high-power devices with VC–relativistic vircators[4] and ion acceleration systems.[2]

Analyzing REBs, it is necessary to take into account effects being insignificant for weakly relativistic beams, in particular, the influence of the self-magnetic field of the REB that effects considerably on the VC dynamics in case of ultra-relativistic electron beams.[8] Therefore, the 3D fully electromagnetic self-consistent model of REB dynamics is required for accurate and correct analysis of the generation processes in this case. Here, we report the results of 3D numerical electromagnetic study of the microwave radiation power of the relativistic vircator system with the annular REB in the presence of an external finite uniform axial magnetic field.

The model under study consists of the finite-length cylindrical waveguide region (electron beam drift chamber) with length L, radius R, and grid electrodes at both ends. An axially symmetrical monoenergetic annular relativistic electron beam with the current I, electron energy W_e, radius R_b, and thickness d is injected through the left (entrance) electrode. Electrons can leave the waveguide region by escaping through the right (exit) grid or by touching the side wall of the drift chamber. In the present report by analogy with our Ref. 8, the values of geometric parameters were chosen as following: $L = 40$ mm, $R = 10$ mm, $R_b = 5$ mm, $d = 2$ mm.

a)Electronic mail: KurkinSA@gmail.com

The external uniform magnetic field with induction $B_z = B_0 \in (0, 20)$ kG is applied along the longitudinal axis of waveguide.

The electron beam source is supposed to be magnetically unshielded in the considered model. This assumption means that the external magnetic field in the drift tube is equal to the magnetic field in the electron source region; therefore, the electron beam does not acquire the azimuthal velocity components at the injection plane (in accordance with Busch's theorem[25]). Such magnetic field distribution is typical for the high-power electronics systems, particularly for the magnetically isolated diodes that form high-current REBs.[25]

Time-dependent fully 3D electromagnetic model of REB dynamics based on solving the self-consistent set of Maxwell equations and equations of charged particles motion accompanied by corresponding initial and boundary conditions (particle-in-cell method)[8,26] is used in the present paper. The main equations are written as

$$\mathrm{rot}\,\mathbf{E} = -\frac{1}{c}\frac{\partial \mathbf{H}}{\partial t}, \quad \mathrm{rot}\,\mathbf{H} = \frac{1}{c}\frac{\partial \mathbf{E}}{\partial t} + \frac{4\pi}{c}\mathbf{j}, \tag{1}$$

$$\frac{d\mathbf{p}_i}{dt} = \mathbf{E}_i + [\mathbf{p}_i, \mathbf{B}_i]/\gamma_i, \quad \frac{d\mathbf{r}_i}{dt} = \mathbf{p}_i/\gamma_i, \quad i = 1\ldots N, \tag{2}$$

where $\mathbf{E}$ and $\mathbf{H}$ are the electric and magnetic intensities, ρ and $\mathbf{j}$ are the charge and current densities, $\mathbf{r}$, $\mathbf{p}$, $\gamma = (1 - (v/c)^2)^{-1/2}$, $\mathbf{v}$ are the radius vector, impulse, relativistic factor, and velocity of the charged particles, correspondingly. The subscript i denotes the number of particle and N is the full number of particles used to simulate the charged particles beam.

The numerical simulation 3D scheme was developed in Ref. 8 and based on 2.5D model developed in our previous work.[24] The equations of charged particles motion (2) are used for the electron beam simulation and solved numerically by means of Bóris algorithm.[27]

The electromagnetic fields in the drift chamber of REB are obtained by means of the numerical solution of Maxwell's equations (1) in cylindrical geometry on the shifted spatio-temporal meshes.[26,28] The values of steps of spatio-temporal meshes is picked out from the Courant-Friedrichs-Lewy condition.[26,29] The space charge and current densities on the meshes are calculated with the help of the bilinear weighing procedure (PIC-method).[26] To model the electromagnetic power output, we use the approach[24] based on the filling the section of electrodynamical system ($L < z < 1.2L$) with the conducting medium with the conductance σ.

Fig. 1 shows the dependencies of the normalized output power of the electromagnetic radiation of REB with VC on the external magnetic field induction obtained with the help of the numerical simulation for two values of the initial electron energy, W_e. One can see that the curves in Fig. 1 demonstrate the same character features as: the presence of three local maxima (which are denoted in Fig. 1 with symbols M_1, M_2, and M_3, respectively). These maxima are shifted towards higher induction values of external magnetic field with the growth of the beam initial energy, W_e.

For the explanation of the physical mechanisms leading to such microwave output power behavior, we consider the obtained dependencies of the REB critical SCL current I_{cr} on

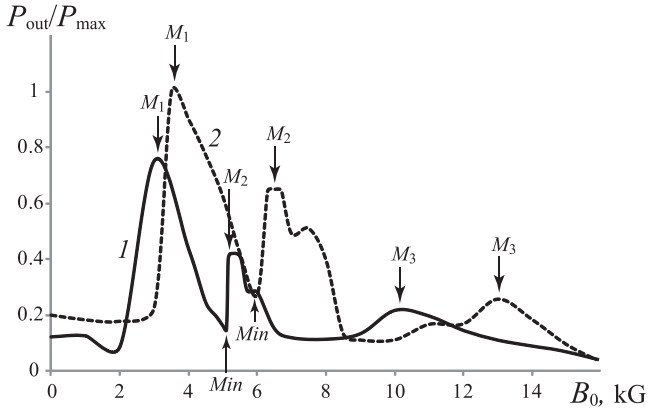

FIG. 1. Dependencies of the normalized output power on B_0 for the following electron beam initial energy values W_e: curve 1 corresponds to 600 keV, 2—850 keV. Beam current $I = 20$ kA; symbols M_1, M_2, and M_3 in figure denote the local maxima of the dependencies.

the external magnetic field induction B_0 shown in Fig. 2 (see Ref. 8). The oscillating VC is known to appear in the system when the beam current exceeds this critical SCL value, I_{cr}. The character dependency of the critical current on the external magnetic field is conditioned by the vortex structure formation in the REB due to the azimuthal instability development under the influence of the beam self-magnetic fields.[8]

To explain the microwave output power behavior, the parameter of the supercriticality $\delta(B_0)$ is useful. The parameter of supercriticality of the electron beam current $\delta(B_0) = I - I_{cr}(B_0)$ is determined by the difference between certain fixed REB current I and the beam critical current $I_{cr}(B_0)$ being the function of external magnetic field induction, B_0. The supercriticality parameter $\delta(B_0)$ characterizes the degree of the VC oscillation development in the REB and depends (for the fixed beam current I) on the magnetic field induction value, B_0. For the fixed beam current, I, and the relatively weak external magnetic fields, the output power of the electromagnetic radiation of the vircator system is a monotone increasing function of the parameter $\delta(B_0)$, i.e., the output power P_{out} increases with the growth of $\delta(B_0)$ in this case.

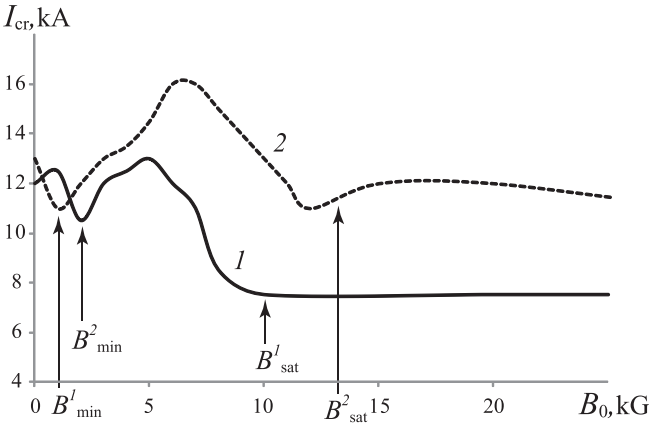

FIG. 2. Dependencies of the REB critical current on the external magnetic field induction value obtained in the work[8] for the following electron beam initial energy values W_e: curve 1 corresponds to 600 keV, 2—850 keV; $B^{1,2}_{min}$ is the value of the magnetic field when the critical beam current reaches the minimal value and $B^{1,2}_{sat}$ is the magnetic field when the curve $I_{cr}(B_0)$ saturates.

Comparing the dependencies $I_{cr}(B_0)$ (Fig. 2) with the dependencies $P_{out}(B_0)$ (Fig. 1) for the corresponding electron beam energy values, one can conclude that the first clearly defined local minimum of $P_{out}(B_0)$ (minima are denoted with symbols "Min" in Fig. 1) is observed for such magnetic field value when the corresponding dependency $I_{cr}(B_0)$ demonstrates the local maximum. Actually, when the critical beam current reaches its maximal value, the parameter of the supercriticality $\delta(B_0)$ for the fixed beam current I ($I = 20\,\text{kA}$ for the case shown in Fig. 1) demonstrates the local minimum and, consequently, the output microwave power obtains the minimal value, too. Analogously, the minima of the dependency $I_{cr}(B_0)$ (Fig. 2) correspond to maximal values of the parameter of the supercriticality and, consequently, to the peaks of the dependence, $P_{out}(B_0)$.

So, the induction of the external magnetic field $B^{1,2}_{min}$, when the dependence $I_{cr}(B_0)$ reaches the first minimum (see Fig. 2)), corresponds approximately to the coordinate of the first maximum M_1 of the dependence $P_{out}(B_0)$. The VC structure is maximally developed for such external magnetic field value. Analogously, the value $B^{1,2}_{sat}$ for which the dependence $I_{cr}(B_0)$ begins to demonstrate the saturation behavior (see Fig. 2) corresponds to the third peak M_3 of the dependence $P_{out}(B_0)$. The tendency of the output power value to decrease with the external magnetic field growth leading particularly to the appearance of the third maximum M_3 is determined by the effect of the beam transverse dynamics suppression in the increasing magnetic field resulting in the lowering of the interaction efficiency of the VC in the electron beam with electromagnetic fields (see Ref. 24).

Let us discuss the physical significance of the discrepancy between the position of the minimum B^1_{min} in Fig. 2 and the maximum M_1 in Fig. 1 for $W_e = 850\,\text{keV}$. In spite of the parameter of supercriticality takes the locally maximal value at $B_0 = 1\,\text{kG}$, the transversal dynamics is great for such external magnetic field. It results in the destruction of the virtual cathode structure and, consequently, the decrease of the output power. At the same time, the transversal dynamics is partially limited and the parameter of supercriticality still takes the low value for the external magnetic field $B_0 = 4\,\text{kG}$. So, the optimal conditions for the virtual cathode radiation mechanisms are established for such external magnetic field and, consequently, the output power is maximal at $B_0 = 4\,\text{kG}$. This effect is more pronounced for the higher values of the beam energy (for $W_e = 850\,\text{keV}$).

Fig. 1 demonstrates the typical dependency of REB radiation output power on the external magnetic field induction and the beam current $P_{out}(B_0, I)$ (Fig. 3) for the considered beam energy value $W_e = 850\,\text{keV}$. One can see that the surface in Fig. 3 demonstrates the presence of the three peak regions (the light gray areas in Fig. 3) stretched along the current axis. The inset in the figure demonstrates the scaled-up region of the second maximum M_2. The position of this peak region M_2 along the magnetic field axis ($B_0 \sim 6 \div 7\,\text{kG}$) depends weakly on the beam current. It is the optimal value of the external magnetic field induction when the REB with VC radiates the output microwave signal with the locally maximal power. One can see that the coordinate of the second maxima M_2 on the output power dependency $P_{out}(B_0)$ for the beam energy $W_e = 850\,\text{keV}$

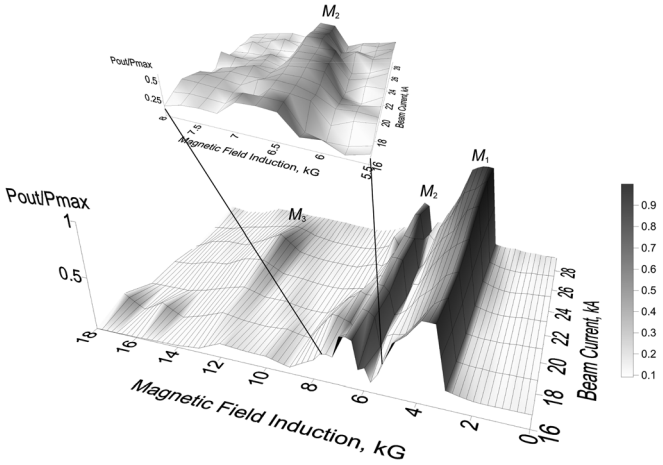

FIG. 3. Dependency of the normalized integral output power of the electromagnetic radiation of REB with VC on the induction of the external magnetic field and the beam current; $W_e = 850\,\text{keV}$; symbols M_1, M_2, and M_3 in figure denote the local maxima of the dependency. The inset demonstrates the scaled-up region of the second maximum M_2.

(Fig. 1, curve 2) corresponds to the optimal external magnetic field, so the output power takes the locally maximal value for such field.

Let us analyze the evolution of the dynamics of the REB in the regime of VC formation with the change of external magnetic field. Figures 4(a)–4(f) show the typical phase portraits of the electron beam which are presented by the projections of the instantaneous positions (black dots in figures) of charged particles of the beam at the transverse plane (r, θ) for the overcritical beam current $I = 20\,\text{kA}$ and the different characteristic values of the external magnetic field, B_0. Fig. 4(a) corresponding to the weak external magnetic field shows the uniform distribution of the REB in the azimuthal direction. One can see that the electron beam demonstrates the formation of different electron structures with the growth of the external magnetic field value. So, the double (Fig. 4(b)), triple (Fig. 4(c)), or single (Fig. 4(d)) vortex electron structures are formed in the REB when the external magnetic field is less than a certain threshold value (9 kG for the case in Fig. 4) due to the development of the so-called azimuthal instability of REB. This instability leading to the loss of axial symmetry of the electron beam dynamics was investigated in detail in the work.[8] It's caused by the mutual influence of the external or self-magnetic fields of the REB, Coulomb's repulsion forces and centrifugal forces on the rotating electrons. The azimuthal instability is developed in the REB (see Ref. 30) when the electrostatic repulsion forces (being proportional to ω_p^2 where ω_p is the plasma frequency of the beam in the VC area) overcome the magnetic restoring forces (being proportional to ω_c^2, where ω_c is the cyclotron frequency).

From the analytical point of view, the condition of the azimuthal instability development means that the frequencies of the fast and slow rotational modes of REB become complex numbers.[30] These frequencies are determined by the following expression:

$$\omega_r^{\pm} = \frac{\omega_c}{2}\left[1 \pm \sqrt{1-\xi}\right], \quad \xi = \frac{2\omega_p^2}{\omega_c^2}, \tag{3}$$

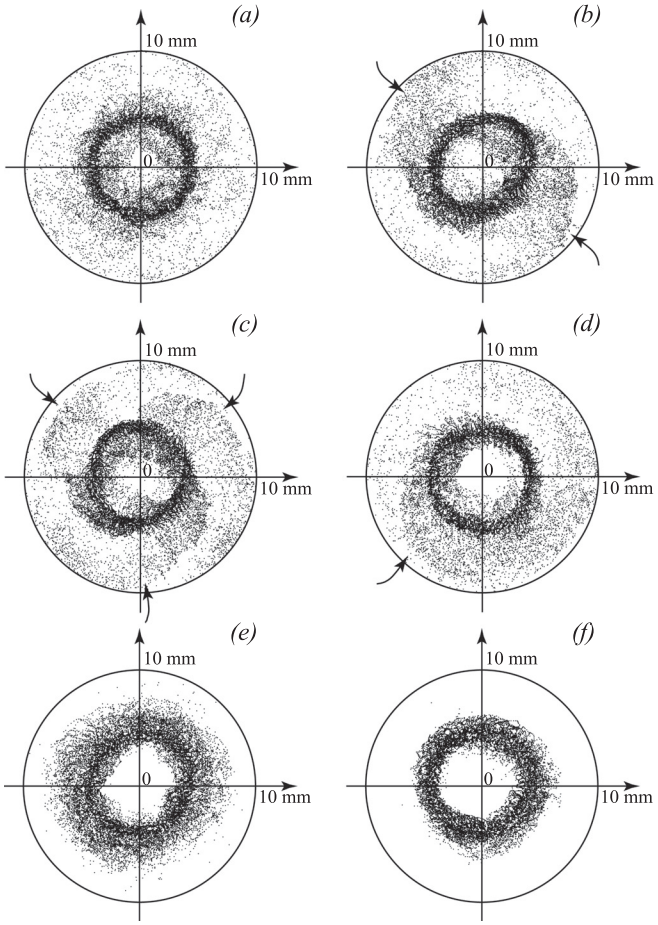

FIG. 4. Projections of the instantaneous positions of the electron beam charged particles at the cutting plane (r, θ) for $B_0 = 3.5$ kG (a), $B_0 = 6$ kG (b), $B_0 = 6.5$ kG (c), $B_0 = 9$ kG (d), $B_0 = 15$ kG (e), and $B_0 = 21$ kG (f); $I = 20$ kA; $W_e = 850$ keV; the longitudinal coordinate of the cutting plane $z_s = 7$ mm. Only particles behind the projection plane ($z < z_s$) are shown in figures; arrows denote the endings of vortex electron structures that are formed in the REB.

where ω_r^+ corresponds to the frequency of the fast rotational mode and ω_r^- corresponds to the frequency of the slow rotational mode. One can see that the frequencies (3) become complex numbers when $\xi > 1$. The estimates have shown that the latter condition of the azimuthal instability is satisfied for the values of external magnetic field induction $B_0 < 9$ kG.

The azimuthal instability is suppressed by the strong external magnetic fields $B_0 > 9$ kG (Figs. 4(e) and 4(f)). The frequencies (3) of both rotational modes become real numbers in this case ($\xi < 1$), and the fast rotational mode corresponds to all electrons gyrating at the cyclotron frequency, whereas the slow rotational mode corresponds to a rotation of the beam as a whole around the symmetry axis.[30] Such external magnetic fields also suppress the transverse dynamics of the REB (Figs. 4(e) and 4(f)).

Fig. 4 shows that the value of the external magnetic field in the range $0 \div 7$ kG determines the structure of the exciting rotational mode and, hence, the shape of the formed electron vortex in the system (cf. Figs. 4(a)–4(d)). This result can explain the existence of the optimal external magnetic field when the output power takes the locally maximal value (maximum M_2 in Fig. 1). It was found out that the interaction efficiency of the VC in the REB with electromagnetic fields and, consequently, the output power are greater when the beam has no nonuniformities in the azimuthal direction. Actually, the case shown in Fig. 4(a) when the REB demonstrates the mostly uniform filling of the drift tube in the azimuthal direction corresponds to the maximal radiation output power (maximum M_1 in Fig. 1, curve *2*). The maximum M_2 is observed for such external magnetic field value when the triple vortex structure is formed in the system (Fig. 4(c)). This structure of the REB in the azimuthal direction is less uniform in comparison with the case shown in Fig. 4(a), therefore, the value of the maximal power in M_2 is less than the value in M_1.

The mostly nonuniform cases of the azimuthal beam dynamics are shown in Figs. 4(b) and 4(d)—double and single vortex structures, correspondingly. As a consequence, the output power takes the minimal values in these cases that correspond to the local minima of the $P_{out}(B_0)$ dependence on the left and right of the maximum M_2, correspondingly. The further growth of the external magnetic field $B_0 > 13$ kG does not lead to the increase of the output power in spite of the suppression of the nonuniform azimuthal structures. It is the consequence of the lowering of the interaction efficiency of the VC in the electron beam with the electromagnetic fields conditioned by the beam transverse dynamics suppression in the increasing magnetic field that was discovered in work.[24] Actually, the strong external magnetic field causes the reflected from VC electrons to move back to the entrance electrode on the trajectories similar to the trajectories of electrons moving from the injection plane to the VC. So, the total energy that the electron beam gives to the electromagnetic fields in such motion and, hence, the output power is low. The double peak behavior of the second maximum M_2 is the consequence of the fine regime switching of the REB dynamics when the external magnetic field is changed in its area.[31]

So, the obtained results explain some features of the dependencies of the vircator output power on the external magnetic field value that were obtained experimentally in Ref. 17. One can see that the curves in Fig. 1 demonstrate the same character features as in the experimental studies (see the typical output microwave power dependencies on the external magnetic field in Table in Ref. 17): the presence of the local maxima and the saturation of the output power value in the low level for the strong external magnetic fields.

We thank Professor I. I. Magda for the fruitful discussion of the obtained results. This work has been supported by The Ministry of education and science of Russian Federation (Project Nos. 14.B37.21.0764 and 14.B37.21.1171); the Russian Foundation for Basic Research (Project Nos. 12-02-00345, 12-02-90022, 12-02-33071, and 13-02-90406); and the President's program (projects MD-345.2013.2 and MK-818.2013.2).

[1]D. J. Sullivan, J. E. Walsh, and E. A. Coutsias, *Virtual Cathode Oscillator (Vircator) Theory*, High Power Microwave Sources Vol. 13 (Artech House Microwave Library, NY, 1987).
[2]A. E. Dubinov and V. D. Selemir, J. Commun. Technol. Electron. **47**, 575 (2002).
[3]Yu. A. Kalinin, A. A. Koronovskii, A. E. Hramov, E. N. Egorov, and R. A. Filatov, Plasma Phys. Rep. **31**, 938–952 (2005).

[4]J. Benford, J. A. Swegle, and E. Schamiloglu, *High Power Microwaves* (CRC Press, Boca Raton, 2007).
[5]D. Biswas, Phys. Plasmas **16**, 063104 (2009).
[6]R. A. Filatov, A. E. Hramov, Y. P. Bliokh, A. A. Koronovskii, and J. Felsteiner, Phys. Plasmas **16**, 033106 (2009).
[7]G. Singh and C. Shashank, Phys. Plasmas **18**, 063104 (2011).
[8]A. E. Hramov, S. A. Kurkin, A. A. Koronovskii, and A. E. Filatova, Phys. Plasmas **19**, 112101 (2012).
[9]R. A. Mahaffey, P. A. Sprangle, J. Golden, and C. A. Kapetanakos, Phys. Rev. Lett **39**, 843 (1977).
[10]S. C. Burkhart, R. D. Scarpetty, and R. L. Lundberg, J. Appl. Phys. **58**, 28 (1985).
[11]R. F. Hoeberling and M. V. Fazio, IEEE Trans. Electromagn. Compat. **34**, 252–258 (1992).
[12]L. A. Bogdankevich and A. A. Rukhadze, Sov. Phys. Usp. **14**, 163 (1971).
[13]W. Jiang, K. Masugata, and K. Yatsui, Phys. Plasmas **2**, 982–986 (1995).
[14]A. Y. Ender, V. I. Kuznetsov, and H. Schamel, Phys. Plasmas **18**, 033502 (2011).
[15]K. G. Kostov, N. A. Nikolov, I. P. Spassovsky, and V. A. Spassov, Appl. Phys. Lett. **60**, 2598–2600 (1992).
[16]K. G. Kostov and N. A. Nikolov, Phys. Plasmas **1**, 1034–1039 (1994).
[17]N. N. Gadetskii, I. I. Magda, S. I. Naisteter, Yu. V. Prokopenko, and V. I. Tchumakov, Plasma Phys. Rep. **19**, 273 (1993).
[18]W. Jiang, H. Kitano, L. Huang, K. Masugata, and K. Yatsui, IEEE Trans. Plasma Sci. **24**, 187 (1996).
[19]K. G. Kostov, I. G. Yovchev, and N. A. Nikolov, Electron Lett. **35**, 1647–1648 (1999).
[20]H. A. Davis, R. D. Fulton, E. G. Sherwood, and T. J. T. Kwan, IEEE Trans. Plasma Sci. **18**, 611–617 (1990).
[21]L. Li, G. Cheng, L. Zhang, X. Ji, L. Chang, Q. Xu, L. Liu, J. Wen, C. Li, and H. Wan, J. Appl. Phys. **109**, 074504 (2011).
[22]T. J. T. Kwan and H. A. Davis, IEEE Trans. Plasma Sci. **16**, 185–191 (1988).
[23]H. A. Davis, R. R. Bartsch, T. J. T. Kwan, E. G. Sherwood, and R. M. Stringfield, IEEE Trans. Plasma Sci. **16**, 192 (1988).
[24]E. N. Egorov and A. E. Hramov, Plasma Phys. Rep. **32**, 683–694 (2006).
[25]S. E. Tsimring, *Electron Beams and Microwave Vacuum Electronics* (John Wiley and Sons, Inc., Hoboken, NJ, 2007).
[26]C. K. Birdsall and A. B. Langdon, *Plasma Physics via Computer Simulation* (Taylor and Francis Group, NY, 2005).
[27]J. P. Boris and K. V. Roberts, J. Comput. Phys. **4**, 552–571 (1969).
[28]T. M. Antonsen, A. A. Mondelli, B. Levush, J. P. Verboncoeur, and C. K. Birdsall, Proc. IEEE **87**, 804–839 (1999).
[29]P. J. Rouch, *Computational Fluid Dynamics* (Hermosa Publishers, Albuquerque, 1976).
[30]R. C. Davidson, *Theory of Nonneutral Plasmas* (W.A. Benjamin, Inc., Advanced book program, Reading, Massachusetts, 1974).
[31]S. A. Kurkin, A. E. Hramov, and A. A. Koronovskii, "The regime switching and the pattern formation in the relativistic electron beam with virtual cathode in the external magnetic field," Phys. Plasmas (to be published).